Surface Science 604 (2010) 1254–1260

Contents lists available at ScienceDirect

Surface Science

journal homepage: www.elsevier.com/ locate/susc

Silver sulphide growth on Ag(111): A medium energy ion scattering study

A.J. Window [a], A. Hentz [a], D.C. Sheppard [a], G.S. Parkinson [a], D.P. Woodruff [a,*], T.C.Q. Noakes [b], P. Bailey [b]

[a] Physics Department, University of Warwick, Coventry CV4 7AL, UK
[b] STFC Daresbury Laboratory, Warrington WA4 4AD, UK

ARTICLE INFO

Article history:
Received 22 February 2010
Accepted 12 April 2010
Available online 18 April 2010

Keywords:
Medium energy ion scattering (MEIS)
Molecule–solid reactions
Corrosion
Compound formation
Silver
Sulphur
Sulphides

ABSTRACT

The interaction of S_2 with Ag(111) under ultra-high vacuum conditions has been investigated by medium energy ion scattering (MEIS). 100 keV He^+ MEIS measurements provide a direct confirmation of a previous report, based on thermal desorption, that the growth of multilayer films of Ag_2S occurs through a continuous corrosion process. These films show a commensurate $(\sqrt{7}\times\sqrt{7})R19°$ unit mesh in low energy electron diffraction, consistent with the epitaxial growth of (111) layers of the high-temperature F-cubic phase of Ag_2S. The substantial range of co-existing film thicknesses found indicates that the growth must be in the form of variable-thickness islands. The use of 100 keV H^+ incident ions leads to a very rapid decrease in the sulphide film thickness with increasing exposure that we attribute to an unusual chemical leaching, with implanted H atoms interacting with S atoms and desorption of H_2S from the surface.

1. Introduction

Adsorption at surfaces can lead to a range of strongly-bonded structural phases including chemisorbed overlayers, substitutional surface alloys, and surface compound phases in which adsorbate and substrate atoms intermix to form a local compound with a well-defined limited thickness. In a few cases, however, interaction with atoms or molecules from the surrounding gas or solution can lead to the formation of bulk compounds that have a well-defined epitaxial relationship to the underlying bulk substrate. Few of these special 'corrosion' systems have been studied in detail, in part because the methods of surface science, which specifically exploit surface specificity, are ill-suited to investigate these systems beyond the very earliest stages of compound formation. Medium energy ion scattering (MEIS) [1], typically using ~100 keV H^+ or He^+ incident ions, is a technique that can be used to explore both true surface phenomena (occurring in the outermost one or two atomic layers of a solid) but also to investigate the sub-surface region to thicknesses of a few hundred Ångström units. Here we report on the use of this technique to investigate the interaction of molecular sulphur in the form of S_2 with Ag(111).

Tarnishing of silver objects in the air is a well-known phenomenon that is attributed to silver sulphide formation at the interface between the silver and a thin water surface film containing air-borne sulphur compounds. An early investigation [2] concluded that the interaction of molecular sulphur with single-crystal films of Ag by electron microscopy led to the formation of thick films of acanthite, the monoclinic phase of Ag_2S [3] that is stable at room temperature, and also identified some epitaxial metal–sulphide orientational relationships. However, the vacuum conditions associated with this study were poor. The first relevant ultra-high vacuum (UHV) investigation using modern surface science methods is a study of the interaction of S_2 with Ag(111) by Schwaha et al. [4]. Using low energy electron diffraction (LEED) they showed that at low coverage a 'complex' phase exists, initially attributed to a '$(\sqrt{39}R16.1°\times\sqrt{39}R16.1°)$' unit mesh but more recently proposed to be more properly described in the matrix notation as $\begin{bmatrix} 3.67 & 0.00 \\ 3.00 & 3.50 \end{bmatrix}$ [5]. At a slightly higher coverage LEED revealed a $(\sqrt{7}\times\sqrt{7})R19°$ pattern, but this persists to much higher coverages. Auger electron spectroscopy (AES) showed a limiting ratio of the Ag and peak heights with increasing exposure to S_2, but temperature programmed desorption (TPD) showed that this was due to continuing growth of a compound film of fixed stoichiometry, rather than saturation of the surface at a lower coverage. Based on these observations, they attributed the $(\sqrt{7}\times\sqrt{7})R19°$ pattern to the formation of an epitaxial film of the high-temperature phase of Ag_2S (referred to as the γ-phase in the very limited report of its structure [6]). This bulk structural phase of Ag_2S has been characterised more fully by neutron scattering [7] and confirmed to have a face-centred cubic lattice with a lattice parameter of 6.27 Å. As such the S–S spacing in the (111) plane is 4.43 Å, an almost perfect match to the $\sqrt{(7/3)}$ spacing 4.41 Å required for epitaxial growth on Ag(111) with a $(\sqrt{7}\times\sqrt{7})R19°$ registry mesh.

In addition to these investigations of gas-phase interactions with molecular sulphur, the interaction of gas-phase H_2S, both under UHV conditions [8] and at ambient pressures [9], have been shown to lead to a $(\sqrt{7}\times\sqrt{7})R19°$ ordered surface phase, although it is unclear as to

* Corresponding author.
E-mail address: d.p.woodruff@warwick.ac.uk (D.P. Woodruff).

0039-6028/$ – see front matter © 2010 Elsevier B.V. All rights reserved.
doi:10.1016/j.susc.2010.04.009

whether this treatment can lead to multilayer compound formation. The same surface ordering has been observed by scanning tunnelling microscopy in electrochemical S deposition [10,11], and under these conditions it is clear that at an appropriate potential, multilayer growth can occur.

Despite the ubiquitous nature of the Ag(111)($\sqrt{7}\times\sqrt{7}$)R19°–S phase, and clear evidence from TPD and electrochemical current measurements that multilayer compound formation can be associated with this ordering, there has been only one reported investigation of the structure of this phase, and this was focussed on the earliest stages of multilayer growth [5]. This investigation, using the normal incidence X-ray standing wave (NIXSW) method [12], followed an earlier detailed investigation of the structure of the closely-related Ag(111)($\sqrt{7}\times\sqrt{7}$)R19°–CH_3S phase, [13] which concluded that the methylthiolate induces a reconstruction of the metal surface to yield a surface comprising 3/7 ML CH_3S species and 3/7 ML of reconstructed Ag atoms. This structure (with the methyl radicals omitted) is shown in Fig. 1. The later study of the Ag(111)($\sqrt{7}\times\sqrt{7}$)R19°–S surface [5] concluded that Ag_2S(111) grows on an interface that is rather similar to the thiolate structure, although the relative spacings and coverage of the S and Ag atoms in this region differ from that of the thiol structure (Fig. 2). NIXSW is not well-suited, however, to explore the properties of thicker layers.

Here we present the results of a new MEIS study of this system which provides mainly information on the stoichiometry and morphology of thicker Ag_2S layers up to ~50 Å average thickness. In the process of performing these experiments, however, we identified a novel form of ion-beam-induced modification that appears to be dominated by chemical, rather than kinetic, influence.

2. Experimental details

The experiments were performed at the Daresbury Laboratory UK National MEIS facility [14]. The ion accelerator fitted with a duoplasmatron ion source was used in the present experiments to produce a beam of H^+ or He^+ ions at a nominal energy of 100 keV. Ions scattered from the sample were detected by a moveable toroidal electrostatic analyser, the two-dimensional (2D) detector [15] of which provides 'tiles' of ion counts as a function of both ion energy and scattering angle over limited ranges of each. The general methodology for extracting from these raw data tiles both the scattered-ion/energy spectra at fixed scattering angle, and the angular blocking curves corresponding to scattering from a single atomic species, has been described elsewhere [13,16]. The end-station comprises separate UHV chambers (typical pressures $2–5\times10^{-10}$ mbar) for sample preparation and characterisation, for sample storage, and for the ion scattering experiments, with sample transfer between chambers being achieved under UHV conditions. The Ag(111) sample was prepared *in situ* by the usual cycles of 1 keV argon ion bombardment and annealing to 600 °C until a well-ordered clean surface was obtained as judged by a sharp (1×1) LEED pattern and AES. The Ag_2S overlayers were prepared by the same method as Schwaha et al. [4], namely through the use of a solid-state Pt/Ag/AgI/Ag_2S/Pt electrochemical cell that delivers a flux of almost entirely S_2 molecules [17,18]. The cell was operated at a temperature of ~180 °C with an applied potential of ~150 mV, with an associated pressure rise during operation to 4×10^{-9} mbar, and deposition was onto the Ag surface at room temperature. Auger electron spectroscopy was used to achieve an approximate calibration of the rate of deposition, assuming 'breaks' in the gradient of the S LVV Auger peak intensity as a function of exposure corresponded to completion of atomic layers. On this basis the deposition rate was estimated to be ~0.15 layers of Ag_2S per minute.

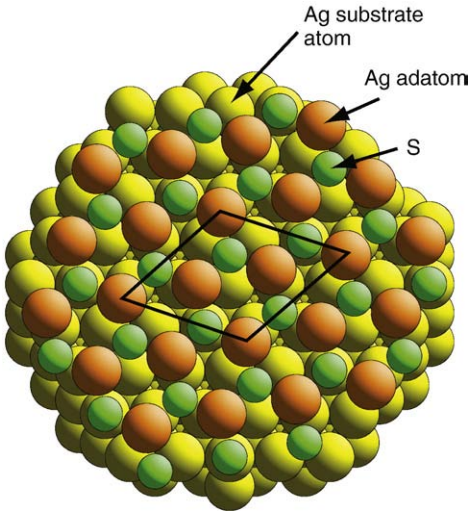

Fig. 1. Model of the ($\sqrt{7}\times\sqrt{7}$)R19° structure formed by methylthiolate, CH_3S–, on Ag (111). The full lines show the unit mesh while the 3/7 ML S headgroup atoms and 3/7 ML Ag adatoms of the reconstructed surface are also shown. This also forms the basis of the model of Ag_2S growth on Ag(111).

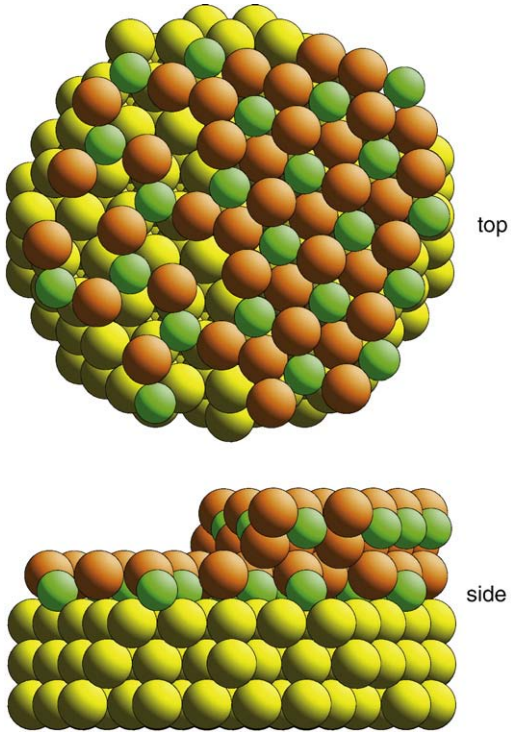

Fig. 2. Top and side views of a model of the early stages of growth of the ($\sqrt{7}\times\sqrt{7}$)R19° structure formed by Ag_2S on Ag(111). On the left is shown an area comprising only the first (2/7 ML) layer of S atoms with 3/7 ML of Ag atoms above, while on the right the first complete Ag_2S layer has grown on top of this interface structure. The Ag_2S is assumed to be a slightly-strained form of the high-temperature F-cubic phase with all Ag atoms in the tetrahedral sites.

3. Sample characterisation and radiation damage

For deposition times of less than ~20 min the LEED pattern was characteristic of the 'complex' phase, only transforming to the expected ($\sqrt{7}\times\sqrt{7}$)R19° pattern at higher coverages. As this exposure is expected, on the basis of the deposition-rate calibration to correspond to an average thickness of ~3 layers, this result is superficially surprising. We note, however, that the 1/7th order diffraction beams that characterise the ($\sqrt{7}\times\sqrt{7}$)R19° pattern are also a sub-set of the diffracted beams of the complex phase, so the continued appearance of the diffraction pattern of the complex phase simply implies that some fraction of the surface remains at this lower

coverage. The implied inhomogeneity of the film, with island growth of the sulphide compound, is consistent with the MEIS data as shown in the following section.

An important issue in any MEIS investigation is to assess the scale of possible sample damage as a result of the incident ion beam. While 100 keV H^+ or He^+ ions clearly do cause damage to any surface, through elastic recoil of the surface atoms that scatter the incident ions, the general mode of use of MEIS ensures that the total number of incident ions used in collecting the data is small enough that there is a low probability that a second ion will scatter from exactly the same atomic position. Nevertheless, the problem is potentially more serious in a compound surface. One problem is the effect of atomic mixing, due to recoil scattering and the subsequent collision cascade, which is more significant in a compound than in an elemental solid. Moreover, the possibility of additional damage (atomic displacements, vacancy creation) through electronic excitations is not an issue in, for example, a metal surface. Typically, MEIS spectra for each 'tile' are recorded using a total incident ion beam dose of 2–4 μC, with a spot size on the sample ~0.5 mm^2, corresponding to ~$2–4\times10^{13}$ ions mm^{-2}.

Damage can manifest itself in the MEIS spectra in one of two ways. Firstly, for simple adsorbate systems, sputtering of the adsorbate species will manifest itself in a decrease in the scattered-ion signal from the adsorbate with increasing exposure to the incident beam. Sputtering, however, has a very low cross-section for 100 keV H^+ and He^+ ions. More generally, damage can lead to crystalline disorder in regions close to the ion impact, and as we use a well-defined low-index crystalline incidence direction in MEIS to achieve surface specificity through sub-surface shadowing, surface damage can lead to sub-surface atoms that should be shadowed becoming visible to the incident beam. The consequence of this is that the 'surface peak' in the scattered-ion/energy spectra, corresponding to scattering from the illuminated atoms at the crystalline surface develops a low energy 'tail' of increasing intensity due to scattering from the sub-surface atoms that become illuminated by their displacements. The ions scattered from these sub-surface atoms emerge at a lower energy due to inelastic energy loss on their passage through the near-surface layers of the solid.

In general we expect significantly less damage to arise from the use of H^+, rather than He^+, incident ions, because the lower mass means that the ions have less momentum at the same kinetic energy and result in less energy transfer in the initial collision with a surface atom. However, in the present case, 100 keV H^+ scattering gave rise to an unusual manifestation of damage at a rather high rate. Fig. 3 shows the results of the experiments conducted to characterise this effect on a sample prepared by an 80 min dose of S_2, leading to a sulphide layer thickness of ~45 Å (see below). Individual 'tiles' of scattered-ion detection around the energy of the Ag scattering surface peak were recorded sequentially, from a sulphided surface, each using only

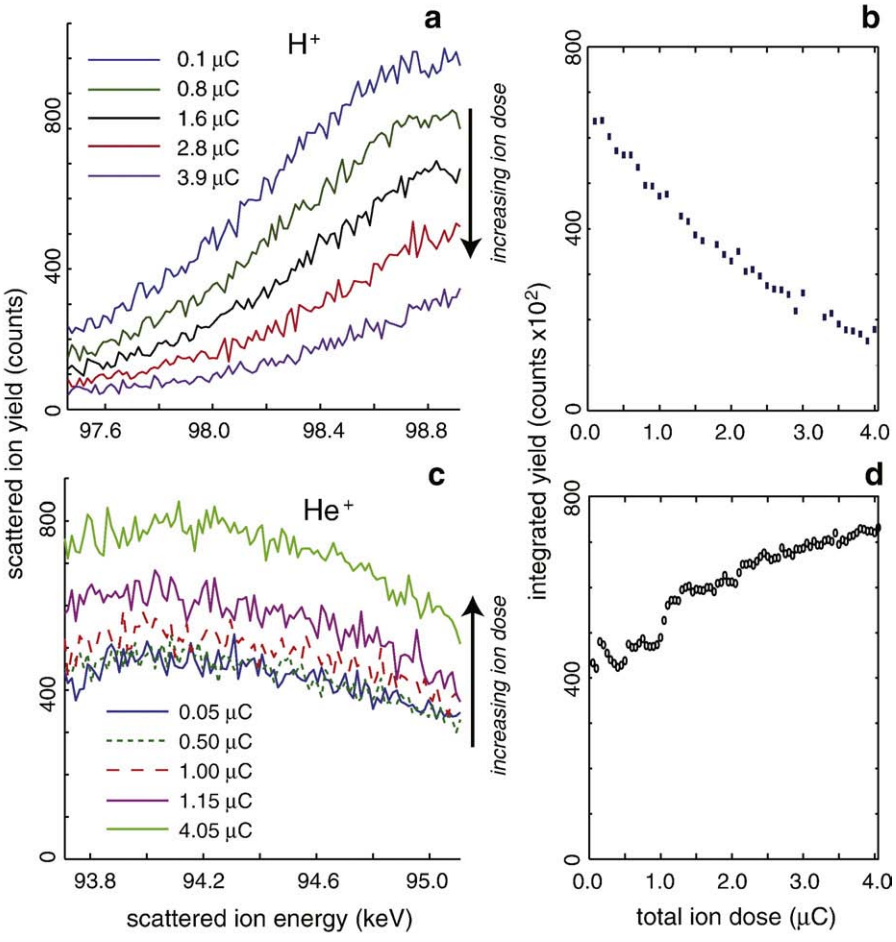

Fig. 3. Results of experiments to determine the effects of radiation damage on an Ag_2S film grown on Ag(111). (a) shows a series of scattered-ion/energy spectra recorded around the Ag surface peak for increasing accumulated ion flux. Each spectrum was recorded in [$\bar{1}$10] incidence around a scattering angle of 75° using 0.1 μC of 100 keV H^+ incident ions. The spectra shown are taken from 2D energy-angle detector 'tiles' projected onto the energy axis with no 'kinematic' energy correction. (b) shows the dependence of the total number of detected ions over the whole detector as a function of accumulated ion dose. (c) and (d) show similar data for 100 keV He^+ scattering but using only 0.05 μC of incident ion flux to record each detector 'tile'.

0.1 μC of incidence flux. This experiment was conducted using incidence along [1̄10], a low-index crystallographic direction of the Ag(111) substrate that nominally only illuminates the outermost Ag layer of the substrate; the detector was centred around a scattering angle of 75°. Notice, though, that the different orientation and structure of the epitaxial Ag_2S film mean that no shadowing is expected within the film, so all Ag atoms within this film should be visible to the incident ion beam. In Fig. 3(a) data from a series of these 'tiles', integrated in angle and projected onto the energy axis, are shown for increasing accumulated beam flux. Notice that because of the very small number of scattered ions detected in this small amount of incident flux, these spectra are not conventional scattered-ion/energy spectra, as no correction has been applied for the change in scattered energy with scattering angle (the so-called 'kinematic factor'). These data clearly show that a very significant (~20%) *decrease* in the Ag scattering signal occurs after less than 1 μC of incident flux. Fig. 3(b) summarises this time dependence as a plot of the integrated scattered-ion signal across the whole detector 'tile' as a function of accumulated incident flux. A total flux of only 0.5 μC is sufficient to lead to a 10% reduction in the signal, clearly indicating that it would be impossible to collect good quality MEIS data from this sample using 100 keV H^+ ions. Fig. 3 ((c) and (d)) shows the result of a similar experiment conducted with 100 keV He^+ incident ions. As *more* damage is to be expected using a He^+ beam, these data were collected using only 0.05 μC of incident flux per measurements, but in fact the change in yield with time is actually much *lower*. Moreover, in this case, the scattered-ion flux around the Ag surface peak increases with increasing accumulated incident flux.

As mentioned above, an increased scattering flux is to be expected if sub-surface atoms are displaced by the incident beam, so the results of the He^+ beam damage experiment are qualitatively consistent with expectations. By contrast, the results of the H^+ scattering experiment are more surprising. The reduction in Ag scattering signal with increased incident flux implies that the Ag_2S film is becoming thinner, the released Ag atoms presumably being accommodated at the metal/sulphide interface into crystalline Ag(111); in effect one has homoepitaxial growth of Ag(111) on Ag(111) at the sulphide interface. The clear implication is that S is lost from the surface, although the MEIS scattering peak from the S atoms is too weak and has too poor a signal-to-noise ratio to provide a direct method of monitoring this loss directly. We attribute this to a *chemical* effect. It seems unlikely that the effect is due to direct interaction of the S atoms with the energetic incident or scattered H^+ ions (or similarly energetic neutralised H atoms), but as these ions and atoms loose energy they become implanted in the sub-surface region. The embedded atomic H can then diffuse rapidly through the metallic sub-surface and sulphide film to the surface where they can combine with S atoms to form H_2S that will desorb. We note that even at room temperature the diffusion coefficient for hydrogen in Ag is extremely high ($D = 2\times10^{-7}\,cm^2\,s^{-1}$ [19]) so in a time $t = 1$ s the diffusion length x, given by the simple formula $x^2 = Dt$; is 4.5 μm, significantly longer than the incident ion range. This availability of thermal H atoms at the interface is thus limited only by the incident ion arrival rate, and not by the diffusion process. The fact that earlier experiments investigating the interaction of H_2S with Ag(111) showed no evidence of multilayer sulphide growth, nor of intact H_2S adsorbed on the surface at room temperature, would seem to support this idea of H_2S formation and desorption from the 'bulk' sulphide.

From the point of view of the experiments reported here, the main conclusion to emerge from this assessment of radiation damage is that MEIS studies from the Ag(111)/Ag_2S system are challenging, but that 100 keV He^+ scattering certainly offers more chance of a successful outcome than the use of 100 keV H^+ ions. Even assuming a level of damage of 10% is acceptable, obtaining useful detailed blocking curves is difficult. Because the energy of the Ag scattering peak depends more strongly on scattering angle for He^+ scattering, it proved necessary to collect four different energy 'tiles' from which to construct a single blocking curve over the 24° angular range that can be extracted from a single detector position. A total ion dose of 1 μC, constrained by the rate of damage, thus leads to only 0.25 μC per tile. Several repeats of these measurements, recorded from different positions on the sample, therefore proved necessary to obtain useful results. Notice that the scattering cross-section scales as the square of the atomic number of the target atom, so recording useful blocking curves from S scattering (a factor of 8.6 weaker) is clearly unrealistic. Despite these severe constraints, some valuable information on the properties of the Ag_2S films could be obtained, as reported in the following section.

4. Results

4.1. Scattered-ion/energy spectra

Fig. 4 shows the results of 100 keV He^+ scattering from the Ag(111) surface, after increasing doses of molecular S_2, in the form of scattered-ion/energy spectra. The data were collected in the double-alignment geometry of [1̄10] incidence and [21̄1̄] detection that minimises the contribution from scattering of sub-surface Ag atoms in the crystalline substrate. The very sharp Ag scattering peak from the clean surface is consistent with this well-aligned scattering geometry. With increasing S_2 dose a lower-energy S scattering peak appears and the Ag scattering peak grows in intensity and width, all consistent with the formation and increasing thickness of a thin film of a material containing both Ag and S with the associated atoms not being aligned to the rows of Ag atoms within the underlying substrate.

The exact shape of these peaks depends on the distribution of film thicknesses in the different preparations and can be extracted by the standard peak-fitting software SIMNRA [20] written for Rutherford backscattering data. The full lines superimposed on the spectra in Fig. 4 are the result of this fitting. Note that the S scattering peak is assumed to correspond to exactly the same thickness distribution as the Ag scattering peak with an Ag:S concentration ration of 2:1; the fit is clearly consistent with the expected Ag_2S stoichiometry. The average film thicknesses and FWHM (full-width half-maximum)

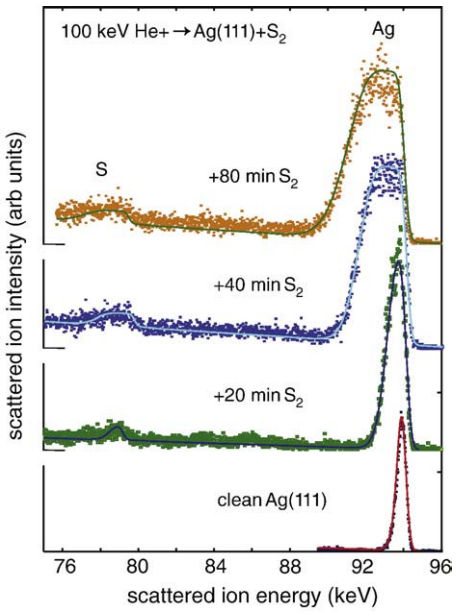

Fig. 4. 100 keV He^+ scattered-ion/energy spectra from Ag(111) after increasing doses of molecular S_2 recorded in a double-alignment geometry of [1̄10] incidence and [21̄1̄] detection. The full lines are fits to the experimental data.

Table 1
Average thickness and FWHM (full-width half-maximum) of the thickness distribution of Ag_2S films extracted from the scattered-ion/energy spectra of Fig. 4 using the SIMNRA program, and average thickness obtained from the blocking curves of Fig. 6 using VEGAS.

Preparation: S_2 dose (min.)	Average thickness (SIMNRA) (Å)	FWHM of thickness distribution (SIMNRA) (Å)	Average thickness (VEGAS) (Å)
20	16.3	12.0	13.5
40	36.2	30.0	36.2
80	46.5	31.9	43.4

distribution of thicknesses used in the SIMNRA simulations shown in Fig. 4 are summarised in Table 1. These spectral fits and the associated tabulated parameters provide clear confirmation of the fact that continued S_2 dosing on the Ag(111) surface in vacuum does, indeed, lead to continued growth of 'bulk' Ag_2S. In addition, the wide distribution of film thicknesses seen in Table 1 provides further confirmation of the 'island' growth behaviour, as indicated by the persistence of the 'complex' LEED pattern for a sulphide film that is several layers thick. Note that the (111) interlayer spacing in bulk (unstrained) F-cubic Ag_2S is 3.62 Å, so a thickness of 16.3 Å (Table 1) corresponds to 4.5 layers.

4.2. Blocking curves

In general MEIS can provide rather detailed crystallographic information through the use of 'blocking curves' — measurements of the scattered-ion signal from a particular atomic species as a function of scattering angle. The system studied here, however, is less well-suited to the application of this approach. There are two underlying problems. The first is that, in order to ensure that the scattering signal from the Ag(111) substrate does not swamp the signal from the sulphide layer, it is necessary to perform the measurements using an incidence direction that corresponds to a shadowing direction of the substrate. Because of the azimuthal twist between the close-packed directions in the surface of the substrate and overlayer, however (Fig. 5) any bulk incident shadowing direction (other than normal incidence) does not correspond to an atomic plane within the sulphide overlayer, so no blocking effects are expected within the overlayer. The second problem relates to the problem of radiation damage which precludes detailed measurements of weak scattering signals. For example, one would like to measure blocking curves in an azimuth corresponding to an atomic plane of the sulphide overlayer (for one of the rotational domains of the structure) using normal incidence, but all the scattering angles are then large, the scattering signal is weak, and adequate signal-to-noise ratios cannot be achieved. Similar constraints preclude meaningful blocking-curve measurements in any direction for the S scattering signal due to the very weak scattering cross-section.

Our blocking-curve investigation was therefore restricted to measurements using two shadowing directions of the Ag(111) substrate, namely $[\bar{1}10]$ and $[\bar{2}\bar{1}\bar{1}]$, as illustrated in Fig. 5. The results are shown in Fig. 6 for both the clean surface and the three different S_2 doses studied by scattered-ion/energy spectra as reported in the previous section. As expected, all these data show only blocking dips that are characteristic of the underlying Ag substrate. The increased yield of Ag scattering and the absence of any additional blocking dips due to the sulphide is consistent with the structural model, but provides no new further details of the structure. The increase in yield, however, does provide some independent measure of the thickness of the films. In particular, blocking curves in MEIS can be simulated for a specific model

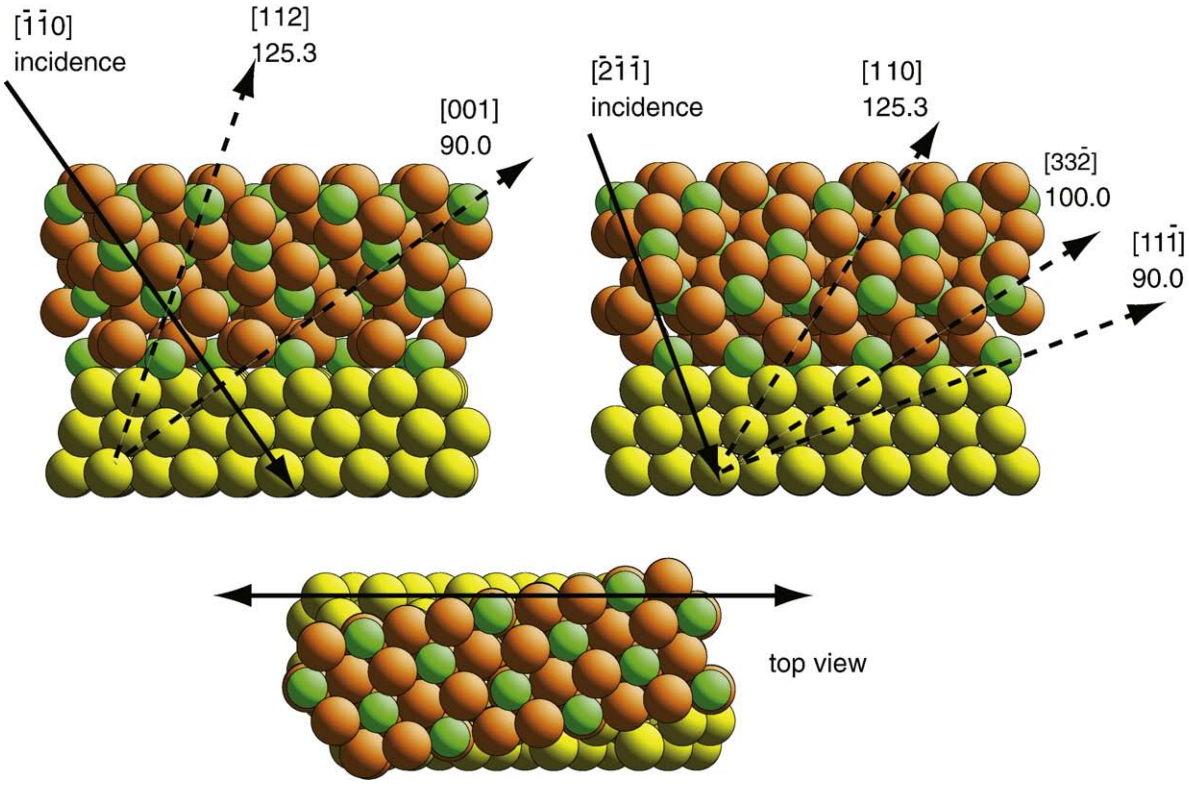

Fig. 5. Diagram showing the $[\bar{1}10]$ and $[\bar{2}\bar{1}\bar{1}]$ incidence geometries used for the blocking curves shown in Fig. 6. The side views of the structure show that even the projection of the atomic positions within the Ag_2S film do not lie in the principle shadowing directions of the substrate, but the top view of the structure also shows that there is an azimuthal twist of the principle directions in the metal and sulphide that ensure this shadowing does not occur. The specific structural model shown here is based on the earlier NIXSW study, but the azimuthal twist is an intrinsic feature of any model having the observed $(\sqrt{7}\times\sqrt{7})R19°$ unit mesh.

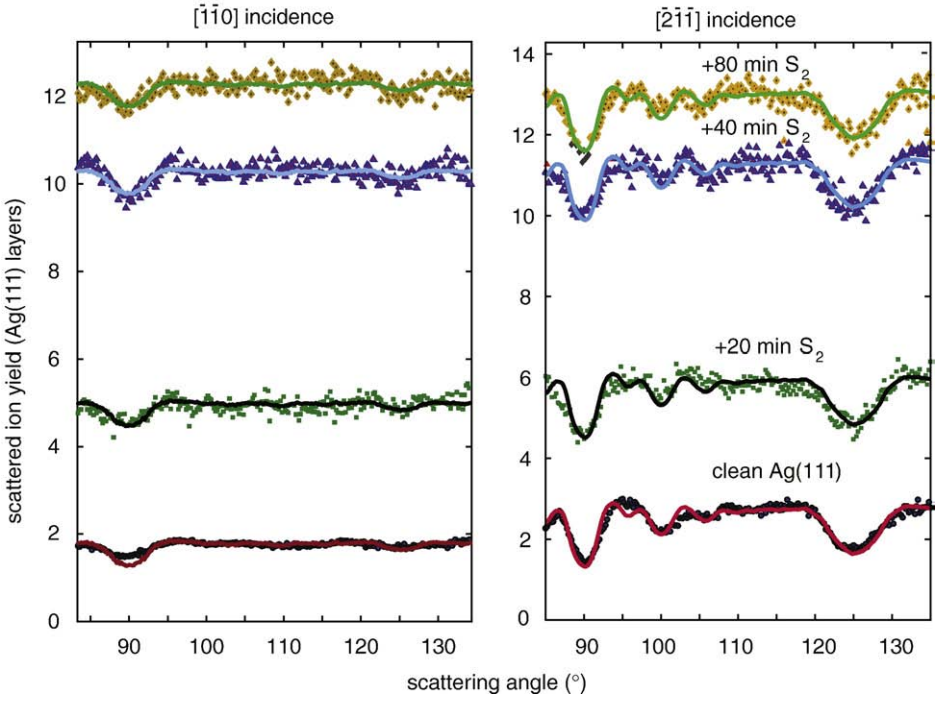

Fig. 6. Blocking curves of the Ag scattering signal from 100 keV He^+ scattering from clean Ag(111) and after increasing doses of S_2 recorded in two different incidence directions (as shown in Fig. 5). The full lines are theoretical fits obtained from a VEGAS calculation as described in the text.

structure using the VEGAS computer program [21]. The model adopted is a clean unrelaxed Ag(111) surface plus an integral number of Ag_2S layers with the interface structure as proposed by Yu et al. [5]. As we are concerned here primarily with an assessment of the absolute number of Ag atoms that are visible to the ion beam in the different structures, appropriate calibration of the experimental yields is essential. To achieve this, measurements were made on a reference sample of Cu shallowly implanted in Si to a known concentration (3.12×10^{15} atoms cm^{-2} with a precision of $\pm3\%$), established independently by conventional Rutherford backscattering.

Using this approach, the simulated blocking curves of Fig. 6 for the two higher S_2 dosing times of 40 and 80 min were obtained with model structures containing 20 and 24 layers of Ag_2S, respectively, corresponding to thicknesses of 36.2 and 43.4 Å. Notice that each Ag_2S layer comprises two Ag layers that 'sandwich' a single S layer, but the number of Ag and S atoms in these atomic layers is only 2/7 the number in an Ag(111) layer. The scattering yields are calibrated in terms of Ag(111) layers. In the case of the film prepared using a 20 min S_2 dose, the fact that the LEED pattern is that of the 'complex' submonolayer sulphided surface means that a model composed of a homogeneous Ag_2S is clearly formally inconsistent, but it is clear from the scattered-ion/energy spectra that much of this surface must be covered with an Ag_2S film. The extra yield seen in the associated blocking curve, relative to that from the clean surface, is 3.2 Ag(111) layers, an increase that would correspond to an average Ag_2S film of 3.7 layers or a thickness of 13.5 Å.

These thickness values are compared with those obtained from the scattered-ion/energy spectra using the SIMNRA program in Table 1. Clearly there is generally a good agreement although the use of the blocking curves to obtain these layer thicknesses provides no information on the distribution of layer thicknesses that is provided by analysis of the scattered-ion/energy spectra. Of course, both methods arise from measurements of the total Ag scattering yield, but the method of calibration is rather different. The VEGAS simulations for the sulphide-covered surfaces also provide formal confirmation of the lack of blocking features introduced by scattering from Ag atoms within the (azimuthally-rotated) sulphide layer.

5. Conclusions

100 keV He^+ MEIS measurements from Ag(111) exposed to increasing fluxes of S_2 molecules under UHV conditions provide a direct confirmation of a previous report that this leads to the growth of multilayer films of Ag_2S through a continuous corrosion process. These films are epitaxial, showing a commensurate $(\sqrt{7}\times\sqrt{7})R19°$ unit mesh, consistent with the growth of (111) layers of the high-temperature F-cubic phase of Ag_2S. The substantial range of co-existing film thicknesses, reflected both by the scattered-ion/energy spectral peak shapes, and by the observation of the 'complex' LEED pattern characteristic of a submonolayer sulphided surface under conditions corresponding to an average film thickness of ~15 Å, clearly indicate that the growth must be in the form of variable-thickness islands. The use of 100 keV H^+ incident ions leads to a very rapid decrease in the sulphide film thickness with increasing exposure that we attribute to an unusual chemical leaching, with implanted H atoms interacting with S atoms and desorption of H_2S from the surface.

Acknowledgements

The authors acknowledge the financial support of the Engineering and Physical Sciences Research Council (UK).

References

[1] J.F. van der Veen, Surf. Sci. Rep. 5 (1985) 199.
[2] M. Shiojiri, A. Maeda, Y. Murata, Jpn. J. Appl. Phys. 8 (1969) 24.
[3] R.W.G. Wyckoff, Second Edition, Crystal Structures, Vol. 1, Interscience Publishers, New York, 1965.
[4] K. Schwaha, N.D. Spencer, R.M. Lambert, Surf. Sci. 81 (1979) 273.
[5] M. Yu, D.P. Woodruff, C.J. Satterley, R.G. Jones, V.R. Dhanak, J. Phys. Chem. C 111 (2007) 3152.
[6] S. Djurle, Acta Chem. Scand. 12 (1958) 1427.
[7] S. Hull, D.A. Keen, D.S. Sivia, P.A. Madden, M.J. Wilson, Phys. Condens. Matter 14 (2002) L9.
[8] G. Rovida, F. Pratesi, Surf. Sci. 104 (1981) 609.
[9] R. Heinz, J.P. Rabe, Langmuir 11 (1995) 506.
[10] G.D. Aloisi, M. Cavallini, M. Innocenti, M.L. Foresti, G. Pezzatini, R.J. Guidelli, Phys. Chem. B 101 (1997) 4774.

[11] V. Brunetti, B. Blum, R.C. Salvarezza, A.J. Arvia, Langmuir 19 (2003) 5336.
[12] D.P. Woodruff, Rep. Prog. Phys. 68 (2005) 743.
[13] M. Yu, D.P. Woodruff, N. Bovet, C.J. Satterley, K. Lovelock, R.G. Jones, V.J. Dhanak, J. Phys. Chem. B 110 (2006) 2164.
[14] P. Bailey, T.C.Q. Noakes, D.P. Woodruff, Surf. Sci. 426 (1999) 358.
[15] R.M. Tromp, M. Copel, M.C. Reuter, M. Horn von Hoegen, J. Speidell, R. Koudijs, Rev. Sci. Instrum. 62 (1991) 2679.
[16] D. Brown, T.C.Q. Noakes, D.P. Woodruff, P. Bailey, Y. Le Goaziou, J. Phys. Condens. Matter 11 (1999) 1889.
[17] C.J. Wagner, J. Chem. Phys. 21 (1953) 1819.
[18] W. Heegemann, K. Meister, E. Bechtold, K. Hayek, Surf. Sci. 49 (1975) 161.
[19] H. Barlag, L. Opara, H. Züchner, J. Alloys Compd. 330–332 (2002) 434.
[20] M. Mayer. http://www.rzg.mpg.de/mam/index.html. SIMNRA Program.
[21] R.M. Tromp, J.F. van der Veen, Surf. Sci. 133 (1983) 159.